Nanotechnology **21** (2010) 015604 (6pp) doi:10.1088/0957-4484/21/1/015604

Au nanoparticle arrays with tunable particle gaps by template-assisted electroless deposition for high performance surface-enhanced Raman scattering

Cheng Mu[1,2], **Jian-Ping Zhang**[3] **and Dongsheng Xu**[1,4]

[1] Beijing National Laboratory for Molecular Sciences, State Key Laboratory for Structural Chemistry of Unstable and Stable Species, College of Chemistry and Molecular Engineering, Peking University, Beijing 100871, People's Republic of China
[2] Functional Nanomaterials Laboratory and Key Laboratory of Photochemical Conversion and Optoelectronic Materials, Technical Institute of Physics and Chemistry, Chinese Academy of Sciences, Zhongguancun Beiyitiao 2, Haidianqu, Beijing 100190, People's Republic of China
[3] Department of Chemistry, Renmin University of China, Beijing 100872, People's Republic of China

E-mail: dsxu@pku.edu.cn

Received 30 September 2009, in final form 28 October 2009
Published 30 November 2009
Online at stacks.iop.org/Nano/21/015604

Abstract
Surface-enhanced Raman spectroscopy (SERS) with enormous enhancements has shown great potential in ultrasensitive detection technologies, but the fabrication of large-scale, controllable and reproducible substrates with high SERS activity is a major challenge. Here, we report the preparation of Au nanoparticle arrays for SERS-active substrates with tunable particle sizes and interparticle gaps, and the enhancement factor of the SERS signal obtained from 4-mercaptopyridine probe molecules was as high as 10^7. The experimental data points show the increase of enhancement factor as a function of the ratio of diameter to interparticle gap, which can be explained by the averaged electromagnetic field enhancement model. Furthermore, we demonstrated that this type of substrate merits its high uniformity, high reproducibility and excellent long-term stability. As the fabrication protocol of such a SERS substrate is simple and inexpensive, this substrate may anticipate a wide range of applications in SERS-based sensors.

(Some figures in this article are in colour only in the electronic version)

1. Introduction

Surface-enhanced Raman spectroscopy (SERS) since its discovery in 1974 gave birth to a powerful new analytical tool that has been the focus of extensive research [1]. SERS is able to enhance the Raman scattering of an analyte by up to a million-fold or more with reference to the normal Raman scattering process. The SERS effect originates primarily from the giant electromagnetic (EM) field resonating with the plasmon at the surface of metal nanostructures (silver, gold, copper, etc), as well as from the chemical enhancement owing to the charge-transfer resonance between the analyte and the substrate [2]. SERS with enormous enhancements has opened up the possibility for single-molecule spectroscopy [3–5] and has shown the great potential in ultrasensitive detection technologies especially for biological molecules and large biostructures [6–13].

One of the keys to widen the application of SERS is to develop highly enhancing substrates for analytical purposes,

[4] Author to whom any correspondence should be addressed.

i.e. for better detection sensitivity to analytes. The modern majority view is that the giant SERS effect primarily results from extraordinarily intense local electromagnetic fields at favorable nanostructure geometries, i.e. the 'hot spot' that is in the interstitial regions or the gaps among closely spaced nanostructures. Theoretical studies of the field enhancement of SERS from metal nanoparticle (NP) arrays predicted the dependence of the enhancement factor on the gap between adjacent NPs [14–16]. For conventional SERS substrates, such as the colloidal clusters of noble metallic NPs or surface-roughened noble metals, the interstitial size is difficult to control owing to the stochastic distribution of the NPs on the substrate. A great deal of research effort in SERS has been focused on the fabrication of controlled and reproducible metallic nanostructures incorporating as much as possible the hot geometries, including the development of various metal architectures, such as dimer-like nanoaggregates [17–20], metal NP arrays by self-organization or nanosphere lithography [21–25] and supported by AAO templates [26, 27], and the closely packed tips of nanowires [28–30]. Recent experimental and theoretical results indicate that the precise control of the gaps among the nanostructures in the regime of sub-10 nm, especially 1–3 nm for optimal coupling of the magnetic field, is critical for the preparation of the SERS substrates with high enhancement factors [31].

In this context, we describe the fabrication and application of a SERS-active substrate consisting of ordered, two-dimensional (2D) arrays of gold NPs on anodic aluminum oxide (AAO) nanochannels with a precisely controlled variation of interparticle gaps, which allow strong SERS signals to be generated from minimal quantities of analytes. The substrates fabricated by our synthetic route are easy to make, stable, reproducible and inexpensive. The results not only open up new possibilities for applying SERS to analytical measurements but also provide important information for improving the fundamental understanding of SERS phenomena.

2. Experimental details

The method used for the preparation of AuNP arrays embedded on an AAO template with self-organized, hexagonally close packed nanochannels is shown schematically in figure 1. First, the high-purity (99.99%) annealed aluminum foil was anodized in 4% oxalic acid aqueous solution in a water bath at 20 °C and 40 V DC for 5 h. To reduce the thickness of the barrier layer (BL) facilitating Ag deposition, secondary anodization was carried out in 0.4 M phosphoric acid at 20 °C and 40 V for 10 min, followed by pore-widening in 0.4 M phosphoric acid at 20 °C for 60 min. Second, silver NPs were grown into the channels of AAO templates by AC electrodeposition at 40 V_{p-p} (sine wave, 50 Hz) using a mixture of 0.05 M $AgNO_3$ and 0.5 M H_3BO_3 as the electrolyte solution with a pH value of 2, set by the addition of sulfuric acid. The AC frequency and time of deposition were chosen so as to form only a small silver particle at the bottom of each pore. Then, the remnant aluminum and the BL were removed by immersion in a $CuCl_2$/HCl solution and 0.4 M phosphoric acid, respectively,

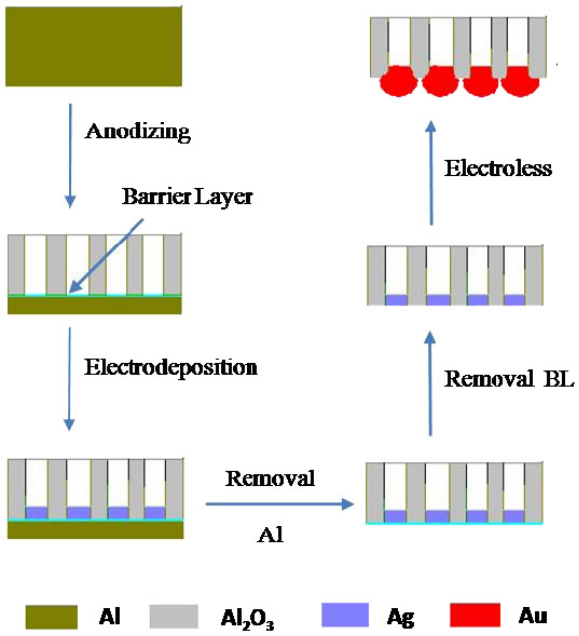

Figure 1. Schematic illustration of the process for fabricating AuNP arrays by templated-assisted electroless deposition.

to expose AgNPs. Finally, the AgNPs on the AAO template were galvanically displaced by Au in the gold-plating bath, a solution of Oromerse part B (Technic Inc.) diluted 1:40 with 0.118 M in Na_2SO_3, 0.68 M in formaldehyde and 0.023 M in $NaHCO_3$, and then the electroless plating of Au continues on the AuNPs owing to their excellent catalytic sites for the reduction of Au(I) to Au(0) [33]. The pH and the temperature are key factors in the Au electroless process. The higher pH plating bath with higher temperature would obviously increase the plating rate. To obtain AuNPs with uniform and smooth surfaces, the appropriate pH and temperature were needed. In the initial period of the electroless process, the temperature of the bath was maintained at 10 °C and the pH of the bath was 10 to hold a moderate plating rate. After the gold particles formed, the temperature was gradually reduced to 3 °C. The AAO templates were placed in the gold-plating bath for different deposition times to obtain AuNPs with various diameters, and meanwhile the interparticle gaps of the AuNPs can be controlled.

Scanning electron microscopy (SEM) images were obtained on an FEI Quanta200 FEG environment microscope. Transmission electron microscopy (TEM) images were obtained on a JEM-2000FX TEM with x-ray energy dispersion analysis equipment (JEOL Company). In order to free individual particles for TEM analysis, the Au–AAO membranes, after annealing at 350 °C in air for 1 h, were dissolved in 1 M NaOH solution for 4 h. UV–vis spectroscopic measurements were performed using a Perkin Elmer Lambda 45 UV/vis spectrometer at room temperature in the range of 400–800 nm. A small piece of template coated with gold particles was placed perpendicular to the light beam inside the cuvette.

For SERS studies, the obtained substrates were immersed in 1 mM 4-mercaptopyridine (4-MP) aqueous solution for

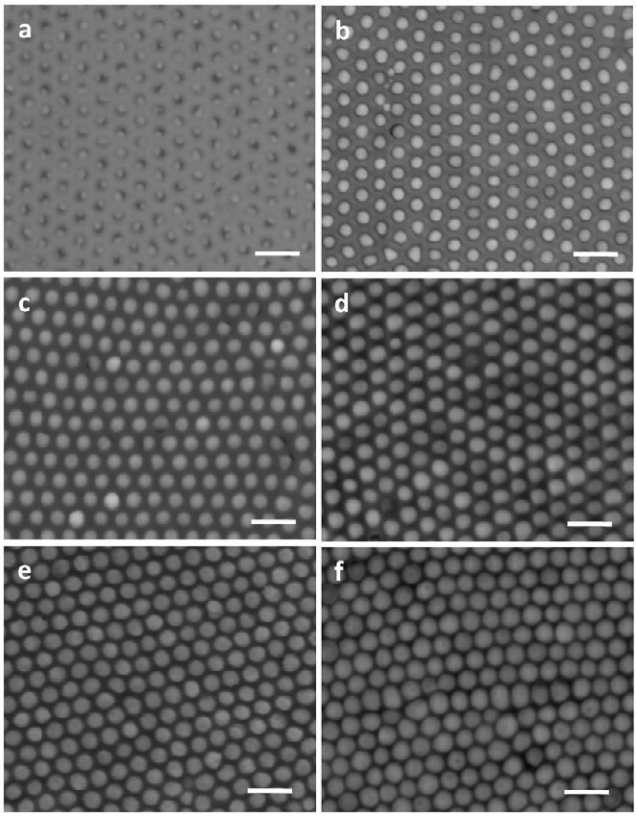

Figure 2. SEM images of AgNP array (a) and the AuNP arrays with different interparticle gaps ((b)–(f)) on the AAO template. The scale bars are 200 nm.

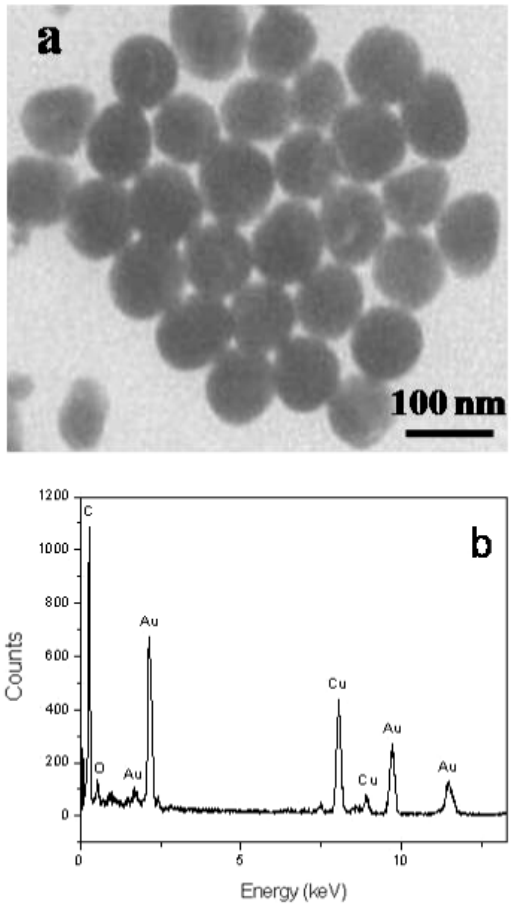

Figure 3. (a) TEM image and (b) EDX spectrum of the AuNPs liberated from the AAO membrane.

24 h to make sure the AuNPs were covered fully with a layer of 4-MP molecules. Then the samples were rinsed with distilled water to remove weakly bounded adsorbates. SERS measurements were made with a Renishaw Ramanscopy 1000 equipped with a 785 nm laser and a Peltier-cooled CCD detector. The laser beam was focused onto a spot 1 μm in diameter and 20 μm in depth.

3. Results and discussion

Figure 2(a) shows the SEM image of a typical 50 nm Ag–AAO membrane that was etched in H_3PO_4 to remove the barrier layer. Nearly each of the AAO channels contains a silver particle with a diameter of ∼45 nm and interparticle gaps of ∼55 nm. The SEM images of AuNP arrays on the AAO surface with different diameters are given in figures 2(b)–(f). The AuNP arrays are hexagonally close packed which is a replica of the AAO nanochannels. The diameters of the AuNPs increase from 50 to ∼90 nm, and the average interparticle gap decreases from 50 to ∼10 nm, as the electroless deposition time of the AuNPs is increased from 5 to about 30 h. The TEM image of gold particles that have been completely liberated from their AAO matrix confirms that the AuNPs are spherical (figure 3(a)) and the energy-dispersive x-ray (EDX) spectrum demonstrates that the AuNPs are only composed of gold (figure 3(b)).

The optical absorption spectrum was used for analyzing the size, shape and aggregation of the AuNPs, as well as the interparticle distance. A series of extinction spectra for the AuNP arrays on the AAO membrane with increasing diameters, i.e. decreasing interparticle gaps, are given in figure 4. In the visible spectral range, the extinction spectra of spherical gold particles with an average size of 3.4 nm or larger are generally dominated by the plasmon band: the peak at around 520 nm is caused by the excitation of surface plasmons (figure 4(a)). As the diameters of the AuNPs increase from 50 to 90 nm, i.e. the gap sizes of the AuNP array decrease from 50 to 10 nm, the extinction peak shifts to the red from 522 to 665 nm (figures 4(b)–(f)). As we know, when the AuNPs begin to aggregate, the extinction peak would redshift towards 750 nm, because of the coupling of the surface plasmon among the closely packed particles. Obviously, no evidence for particle aggregation was observed in these AuNP substrates.

The SERS activity of AuNPs/AAO substrates was demonstrated by applying an aqueous solution (10^{-3} M) of 4-MP to the AuNP array substrate. 4-MP was used as the probe molecule, which can chemically adsorb onto AuNPs in monolayers and align perpendicularly on the Au surface. The spectra of pure 4-MP powders under the excitation wavelength of 785 nm are shown for comparison in figure 5(A)-a. The intense bands at 1093, 1012, 1060 and 1212 cm^{-1} are ascribed

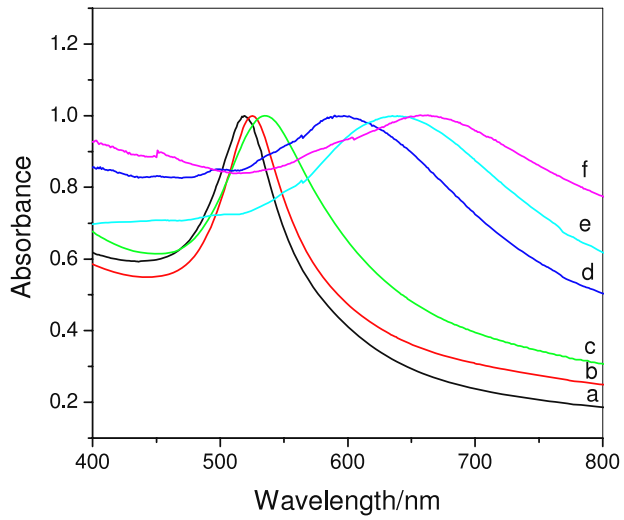

Figure 4. UV–vis absorption spectra of the AuNP arrays with different interparticle gaps: (a) ∼50 nm, (b) ∼40 nm, (c) ∼30 nm, (d) ∼20 nm, (e) ∼15 nm and (f) ∼10 nm.

to the C–S breathing and the fundamental ring vibrations, in good agreement with the documented data [32]. Figures 5(A)-b–(A)-e show the Raman spectra of the AuNPs/AAO samples with interparticle gaps of 30, 20, 15 and 10 nm. As shown in figure 5(A), the Raman peak intensity increases when the gaps of the AuNPs decrease. The intensity of the peak at 1093 cm^{-1} for the 4-MP SERS spectra recorded as a function of the interparticle gap size is shown in figure 5(B). The SERS intensity at 1093 cm^{-1} decreases by a factor of about 200 on going from interparticle gaps of 10 nm to interparticle gaps of 30 nm, which is in agreement with other experimental data on ordered nanoparticle arrays [21]. The strong enhancement can be attributed to the fact that the AuNPs/AAO substrate has a very high density of both AuNPs and 'hot-spots' likely existing among the gaps between neighboring AuNPs [17].

To evaluate the enhancement factors (EF), we compared the ratios of SERS peak intensities of the saturated 4-MP coverage to the corresponding unenhanced signals from a neat 4-MP film of known thickness (20 μm). When the intensities are normalized for laser power and acquisition time, under the same collection conditions, the SERS EF is given by $EF = (I_{SERS}/N_{SERS})/(I_{bulk}/N_{bulk})$, where I_{SERS} and I_{bulk} are the corresponding measured SERS and normal Raman integrated intensity of the 4-MP peak at 1093 cm^{-2}, respectively, while N_{SERS} and N_{bulk} stand for the number of probe molecules (4-MP) on AuNPs under laser illumination and the number of the probe molecules in bulk, respectively. The value of N_{bulk} was readily calculated from the 4-MP bulk density and the Raman scattering volume which is from the Raman scattering area (1 μm × 1 μm) and the 4-MP film thickness (20 μm). The number of 4-MP molecules adsorbed on the AuNP substrate was calculated by assuming a monolayer coverage and a SERS-active area given by the sum of the area of the gold particles in the probed spot (∼1 μm in diameter). The packing density of 6.8×10^{14} molecules cm^{-2} reported for benzenethiol was utilized for N_{SERS} calculation [21, 22]. The EF for the AuNP SERS substrate with a gap of about 10 nm at 785 nm excitation wavelength was at least above 10^7. However, the 4-MP molecule, being a more bulky molecule than benzenethiol, is expected to possess a lower packing density; thus, the SERS enhancement factors reported in this work are lower limits. It is likely that the SERS enhancement factor for the AuNP substrate is due mainly to an electromagnetic dipole effect accentuated by the high ratio of the AuNP diameter to the interparticle gap. In addition, for bigger AuNPs, the wavelength of the plasmon resonance would match better with the 785 nm Raman excitation, subsequently resulting in an increase of the SERS intensity.

The AuNP arrays can also be used for SERS of other molecules which are not chemically attached to a substrate, such as β-carotene. Figure 6 show the SERS spectrum on

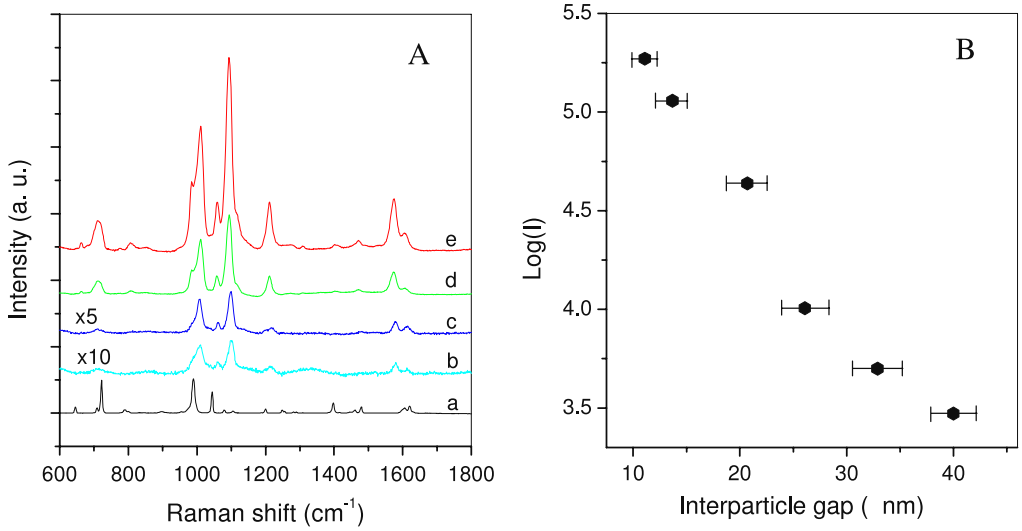

Figure 5. (A) Typical Raman signals from the neat 4-MP films with a thickness of 20 μm (a) and the SERS spectra of monolayer 4-MP molecules on the AuNPs/AAO substrates with interparticle gaps of 30 nm (b), 20 nm (c), 15 nm (d) and 10 nm (e). (B) Experimentally measured intensities of the 1093 cm^{-1} SERS line of 4-MP recorded as a function of the interparticle gap size. The error bars for interparticle gaps are shown for those points for which the error exceeds the size of the point.

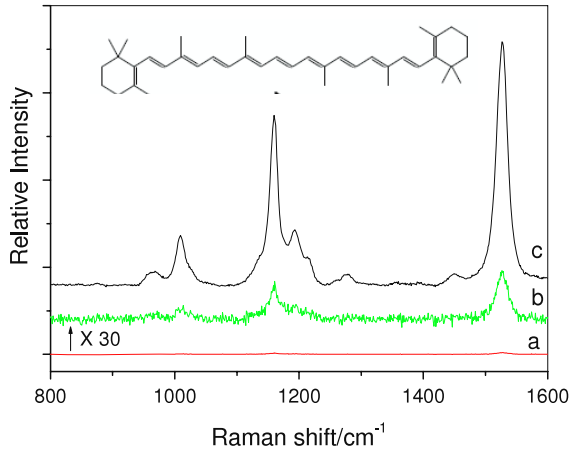

Figure 6. Raman spectrum of β-carotene absorbed on the bare AAO template (curve a) and that magnified by a factor of 30 (curve b). Curve c is the SERS spectrum of β-carotene adsorbed on the AuNP array substrate. Inset shows the molecular structure of β-carotene.

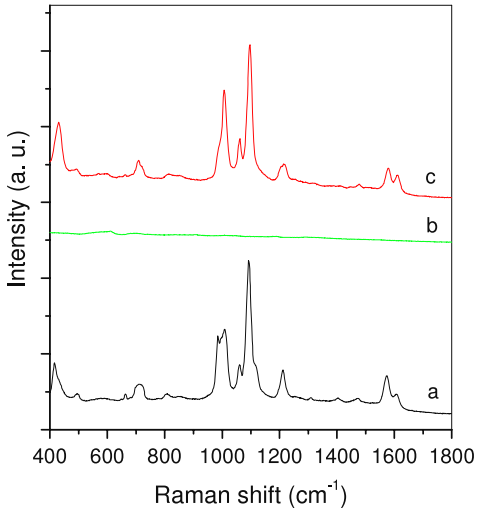

Figure 7. SERS spectra of 4-MP solution (10^{-3} M) on an AuNPs/AAO substrate with a interparticle gap of 10 nm: (a) after 12 months of storage, (b) with the 4-MP molecules desorbed in aqueous hydrogen peroxide solution, and (c) with the 4-MP molecules absorbed again.

AuNP arrays and the normal Raman spectrum on AAO for β-carotene. The Raman spectra with (curve c) and without (curve b) the SERS effect have the same set of Raman shifts as well as similar intensity ratios among Raman lines. In contrast, the SERS intensity increased by a factor of 160 compared to the normal Raman (curve a).

For practical applications, an important requirement of the SERS-active substrate is its long-term stability. Our SERS substrate exhibits a prominent advantage in terms of the stability: after 12 months of storage, the SERS spectrum of 4-MP on the AuNPs/AAO substrate keeps almost the original intensity (figure 7(a)). When the 4-MP molecules were desorbed from the AuNPs/AAO membrane by the use of aqueous hydrogen peroxide solution, the substrate gives

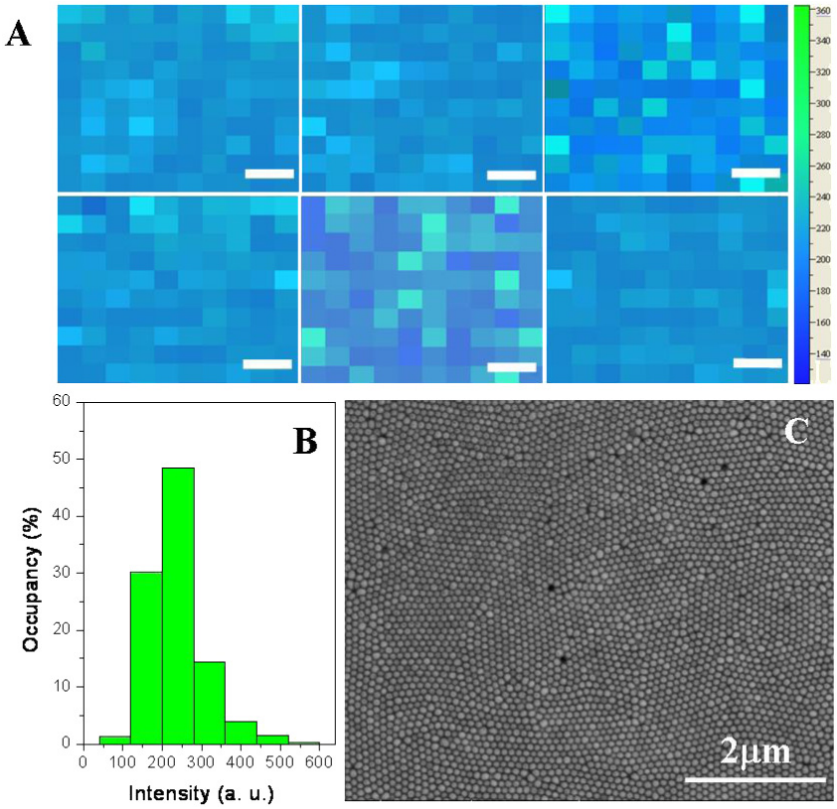

Figure 8. (A) Selected SERS maps of 4-MP molecules (1070–1120 cm^{-1}, 20 × 20 μm^2, step size 2 μm) on the AuNPs/AAO substrate with the average intensities integrated. Scale bar: 4 μm. (B) The histogram of all intensities in (A). (C) A typical SEM image of the AuNP array over a large area.

no obvious Raman response (see figure 7(b)). Meanwhile, when the 4-MP molecules are absorbed again onto the same AuNPs/AAO substrate, the SERS spectra restored both the positions and the peak intensities (see figure 7(c)). After the SERS test, the analyte can be desorbed from the substrates by washing with different solvents such as peroxide, methanol, etc. We found that the SERS activity of the AuNP array substrates was not lost when the substrates were used repeatedly.

Another requirement for the practical usage of the SERS substrate is the uniformity of the substrate in Raman enhancement. Figure 8(A) displays six of the point-by-point SERS maps for different areas (20 μm $\times$ 20 μm) of a SERS substrate, which were recorded with a 2 μm step for the 4-MP molecules on AuNPs. The mapping was obtained using the integrated area of the baseline-corrected peaks at 1093 cm^{-1}, and brighter colors represent higher intensities of the SERS signal. From the histogram in figure 8(B), the Raman maps of figure 8(A) have very narrow intensity distribution, and the majority of the values lie between 150 and 250 counts. In addition, the average intensity of the SERS maps recorded from different areas is quite close, indicating that the AuNPs/AAO substrate is, in general, homogeneous for SERS. Giant enhancement was occasionally observed as indicated by the brightest point with a value of 500 counts in figure 8(A). The small spatial variation in SERS performance could be caused by the spatial inhomogeneity of the AuNPs in dimensions of $\sim$100 nm (figure 8(C)). The reason for the formation of the extremely 'hot' site is attributed to the larger AuNPs in some domain boundaries which result in small interparticle gaps with multipole couplings of neighboring particles. In contrast, both defects and smaller AuNPs may lead to larger interparticle gaps. It is pertinent to compare the homogeneity with discrete nanoparticle systems whose SERS signals may vary a few orders of magnitude, depending on the configurations and incident polarizations [34–36].

4. Conclusions

In summary, we have developed a method for the preparation of AuNP arrays for SERS-active substrates with tunable particle size and interparticle gaps, and the enhancement factor of the SERS signal obtained from the 4-MP probe molecules was as high as 10^7. This type of substrate merits its large SERS enhancement, large area and high uniformity, high reproducibility and excellent long-term stability. As the fabrication protocol of such a SERS substrate is very simple and inexpensive, the AuNP array substrate may anticipate a wide range of applications in SERS-based sensors for rapid, accurate and cost-effective detection of extremely low levels of dyestuff, pollutants and biomolecules.

Acknowledgments

This work is supported by NSFC (grant nos. 20525309, 20673008 and 50821061) and MSTC (MSBRDP, grant nos. 2006CB806102 and 2007CB936201).

References

[1] Fleischmann M, Hendra P J and McQuillan A J 1974 *Chem. Phys. Lett.* **26** 163
[2] Kneipp K, Kneipp H, Itzkan I, Dasari R R and Feld M S 1999 *Chem. Rev.* **99** 2957
[3] Nie S M and Emory S R 1977 *Science* **275** 1102
Tian Z Q, Ren B and Wu D Y 2002 *J. Phys. Chem.* B **106** 9463
[4] Kneipp K, Wang Y, Kneipp H, Perelman L T, Itzkan I, Dasari R R and Feld M S 1997 *Phys. Rev. Lett.* **78** 1667
[5] Xu H, Bjerneld E J, Käll M and Börjesson L 1999 *Phys. Rev. Lett.* **83** 4357
[6] Shafer-Peltier K E, Haynes C L, Glucksberg M R and Van Duyne R P 2003 *J. Am. Chem. Soc.* **125** 588
[7] Graham D, Mallinder B J and Smith W E 2009 *Angew. Chem. Int. Edn* **39** 1061
[8] Fabris L, Dante M, Braun G, Lee S J, Reich N O, Moskovits M, Nguyen T and Bazan G C 2007 *J. Am. Chem. Soc.* **129** 6086
[9] Bell S E J and Sirimuthu N M S 2006 *J. Am. Chem. Soc.* **128** 15580
[10] Braun G, Lee S J, Dante M, Nguyen T, Moskovits M and Reich N 2007 *J. Am. Chem. Soc.* **129** 6378
[11] Moore B D, Stevenson L, Watt A, Flitsch S, Turner N J, Cassidy C and Graham D 2004 *Nat. Biotechnol.* **22** 1133
[12] Shanmukh S, Jones L, Driskell J, Zhao Y, Dluhy R and Tripp R A 2006 *Nano Lett.* **6** 2630
[13] Huang X, El-Sayed I H, Qian W and El-Sayed M A 2007 *Nano Lett.* **7** 1591
[14] García-Vidal F J and Pendry J B 1997 *Phys. Rev. Lett.* **77** 1163
[15] Xu H, Aizpurua J, Käll M and Apell P 2000 *Phys. Rev.* E **62** 4318
[16] Genov D A, Sarychev A K, Shalaev V M and Wei A 2004 *Nano Lett.* **4** 153
[17] Sawai Y, Takimoto B, Nabika H, Ajito K and Murakoshi K 2007 *J. Am. Chem. Soc.* **129** 1658
[18] Michaels A M, Jiang J and Brus L 2000 *J. Phys. Chem.* B **104** 11965
[19] Talley C E, Jackson J B, Oubre C, Grady N K, Hollars C W, Lane S M, Huser T R, Nordlander P and Halas N J 2005 *Nano Lett.* **5** 1569
[20] Nordlander P, Oubre C, Prodan E, Li K and Stockman M I 2004 *Nano Lett.* **4** 899
[21] Lee S J, Guan Z Q, Xu H X and Moskovits M 2007 *J. Phys. Chem.* C **111** 17985
[22] Lombardi I, Cavallotti P L, Carraro C and Maboudian R 2007 *Sensors Actuators* B **125** 353
[23] Wang H H, Liu C Y, Wu S B, Liu N W, Peng C Y, Chan T H, Hsu C F, Wang J K and Wang Y L 2006 *Adv. Mater.* **18** 491
[24] Wang H, Levin C S and Halas N J 2005 *J. Am. Chem. Soc.* **127** 14992
[25] Haynes C L and Van Duyne R P 2001 *J. Phys. Chem.* B **105** 5599
[26] Foss C A, Hornyak G L, Stockert J A and Martin C R 1994 *J. Phys. Chem.* **98** 2963
[27] Hornyak G L, Patrissi C J and Martin C R 1997 *J. Phys. Chem.* B **101** 1548
[28] Schierhorn M, Lee S J, Boettcher S W, Stucky G D and Moskovits M 2006 *Adv. Mater.* **18** 2829
[29] Sauer G *et al* 2006 *Appl. Phys. Lett.* **88** 023106
[30] Lee S J, Morrill A R and Moskovits M 2006 *J. Am. Chem. Soc.* **128** 2200
[31] Lu Y, Liu G L and Lee L P 2005 *Nano Lett.* **5** 5
Fang Y, Seong N H and Dlott D D 2008 *Science* **321** 388
[32] McLellan J M, Xiong Y J, Hu M and Xia Y 2006 *Chem. Phys. Lett.* **417** 230
[33] Wirtz M and Martin C R 2003 *Adv. Mater.* **15** 455
[34] Bosnick K A, Jiang J and Brus L E 2002 *J. Phys. Chem.* B **106** 8096
[35] Xu H X and Käll M 2003 *ChemPhysChem* **4** 1001
[36] Itoh T, Hashimoto K, Ikehata A and Ozaki Y 2003 *Appl. Phys. Lett.* **83** 5557